Lifetime and droplets size distribution of dense sprays

L. Rotily [1] and E. Villermaux [1,2,*]
[1] *Aix Marseille Université, CNRS, Centrale Marseille, IRPHE UMR 7342, 13384 Marseille, France*
[2] *Institut Universitaire de France, 75005 Paris, France*

(Received 23 January 2026; accepted 8 May 2026; published 1 June 2026)

We study the evaporation dynamics of spray lamellae—the paradigm of dense sprays evaporation—injected into a quiescent dry environment from an oscillating source. Lamellae are made of a collection of densely packed microns in size droplets of liquids with different volatilities, initially in equilibrium with their vapor. Building on an earlier study [de Rivas *et al.*, Phys. Rev. Fluids **1**, 014201 (2016)], we confirm that the lifetime of an individual droplet embedded in such a spray is much larger than expected from the usual d-squared law describing the fate of a single isolated droplet evaporating in a quiescent environment. By analogy with the way mixing times of scalars are understood from the coupling between stretching and diffusion, we show that the boundary between the spray and the diluting environment is slaved to the dynamics of its saturating vapor concentration field as envisaged in Villermaux *et al*. [Phys. Rev. Fluids **2**, 074501 (2017)], thus explaining the very substantial evaporation delay of the liquid phase in spite of its division into fine droplets. We quantify the evaporation time for the stirring protocol of an undulating lamellae as well as, thanks to unique *in situ* measurements, the concomitant evolution of the droplets number, and size distribution in the spray.

DOI: 10.1103/ms1r-7jb9

I. INTRODUCTION

A liquid evaporates until it is in equilibrium with its vapor, whose partial pressure is prescribed by temperature only. When a small liquid mass evaporates into a large diluting space, equilibrium is never reached, and the liquid converts into vapor entirely. If this ultimate thermodynamic limit is no longer an issue [1], the kinetics of the equilibration process, namely, the evaporation rate, has received satisfactory answers only partially. The case of a spherical liquid droplet isolated into a quiescent medium with uniform vapor concentration (the relative humidity for water evaporating in air) was historically first considered; this is the famous d-squared law which explains that the liquid evaporation rate at the droplet surface is given by the rate at which the vapor diffuses away from the droplet in inverse proportion to its diameter [2–4]. This configuration has been described with several boundary conditions [5–7], including its early time transient [8], the same problem holding for the growth, or dissolution of bubbles in liquids [9]. The corrections to this law due to a relative motion of the droplet with its surroundings were then envisaged [10], a case relevant to situations where the liquid phase is not passively transported by the phase in which the vapor diffuses [11,12].

Probably because of its simplicity and elegance, the d-squared paradigm remains the starting point of most tudies involving sprays, even in situations where it has no chance to be directly relevant, although these conditions are the rule rather than exceptions. The d-squared law states that the square of the diameter of droplets isolated in a quiescent environment decays linearly in time: $d^2 = d_0^2 - \kappa t$. However, droplets are practically never formed in isolation in nature, and many

*Contact author: emmanuel.villermaux@univ-amu.fr

droplets in close proximity experience a saturated vapor field from their neighbors that obviously hinders their individual evaporation. This fact is well-known for sea spray [13] transported by wind over large distances [14], for most agricultural sprays [15] subjected to persistent drift [16,17], in combustion engines where droplets burn in groups rather than individually [18,19], in clouds where the growth of droplets from nuclei is known to be sensitive to a varying vapor supersaturation field with broad fluctuations [20–23], not to mention the extended lifetime of droplets exhaled from chimneys, cooling towers [24], or humans, both indoors [25,26] and outdoors [27–29], and their associated sanitary consequences [30,31].

Collective effects inducing an evaporation (or condensation) delay compared to the d-squared expectation have been documented in some academic settings [32,33], including the evaporation or condensation of sessile droplets [34,35] and when the substrate in which the vapor dilutes is deformed and stirred [36,37], which is our present topic. These last studies established that the evolution of a densely packed in space dispersion of passively advected droplets is slaved to the dynamics of its saturating vapor field. Describing dense sprays is therefore amenable to a scalar mixing problem [36], the one of the stretching enhanced diffusion of the vapor field in the diluting environment. A fair caricature is that densely packed droplets do not evaporate, but do so promptly (on a timescale given by the d-squared law) as soon as their interstitial vapor concentration falls below the thermodynamic saturating concentration. The lifetime of the spray is thus given by the time it takes for the vapor to evacuate the droplets assembly, and thus coincides with the mixing time of the vapor constructed on the initial size of the droplets packing [37].

The contributions [36,37] just mentioned were both concerned with stirring protocols involving exponential stretching and a single liquid (ethanol in [36] and acetone in [37]). We generalize the description here to a weaker, linear elongation stirring protocol which now involves, for the same stirring flow, liquids with very different volatilities. Also, we monitor the droplets sizes as their assembly evaporates, which allows us to address the fundamental question of the evolution of the droplets size distribution in evaporating dense sprays, and find again a phenomenology markedly different from the d-squared, isolated droplets expectation.

II. CONFIGURATION AND DIAGNOSTICS

A. Stirring protocol

The stirring protocol consists of letting a spray jet be flattened and deflected by a plate oriented at a slight angle, which oscillates perpendicularly to the ejection direction. The resulting spray sheet, whose ejection velocity v is conserved, and whose direction is a periodic function of time (pulsation ω, amplitude α), expands ballistically in its diluting environment at rest, thus producing a linear increase of material lines along the sheet. The perpendicular velocity is $\alpha v \cos \omega t$, the downstream position x of an element of the spray ejected at time t_i is $x \approx v(t - t_i)$, while its perpendicular position is $\alpha v(t - t_i) \cos \omega t_i$. The distance ℓ between two extrema of the element ejected at, say, $\omega t_1 = 0$ and $\omega t_2 = \pi$, is such that $\ell^2 = [\alpha v(t - t_1) \cos \omega t_1 - \alpha v(t - t_2) \cos \omega t_2]^2 + [v(t_2 - t_1)]^2$, that is,

$$\ell \approx \ell_0(1 + \sigma t) \quad \text{with} \quad \sigma = \frac{2}{\pi}\alpha\omega, \tag{1}$$

which is an approximate but convenient crossover formula which interpolates between the initial lamella length $\ell_0 = v\pi/\omega$ and its later time linear elongation $\ell \to 2\alpha v t$. The full mixing problem with the exact kinematics $\ell/\ell_0 = \sqrt{1 + (\sigma t)^2}$ is well-known [38–40] and leads to essentially identical results as those derived in the sequel, the form in Eq. (1) being easier to manipulate. The lamella at time t is located about the downstream position $x = vt$. The sheet envelope increases linearly with the downstream position x. Here is how this protocol is realized practically:

We operate within a large ($35 \times 35 \times 35\,\text{cm}^3$) box safe from draughts, fitted with an inlet for the spray injection, an evacuation outlet on the opposite side (so humidity will not accumulate in the box), and a slit at the top to let a laser sheet shine through (Fig. 1). The spray is formed by

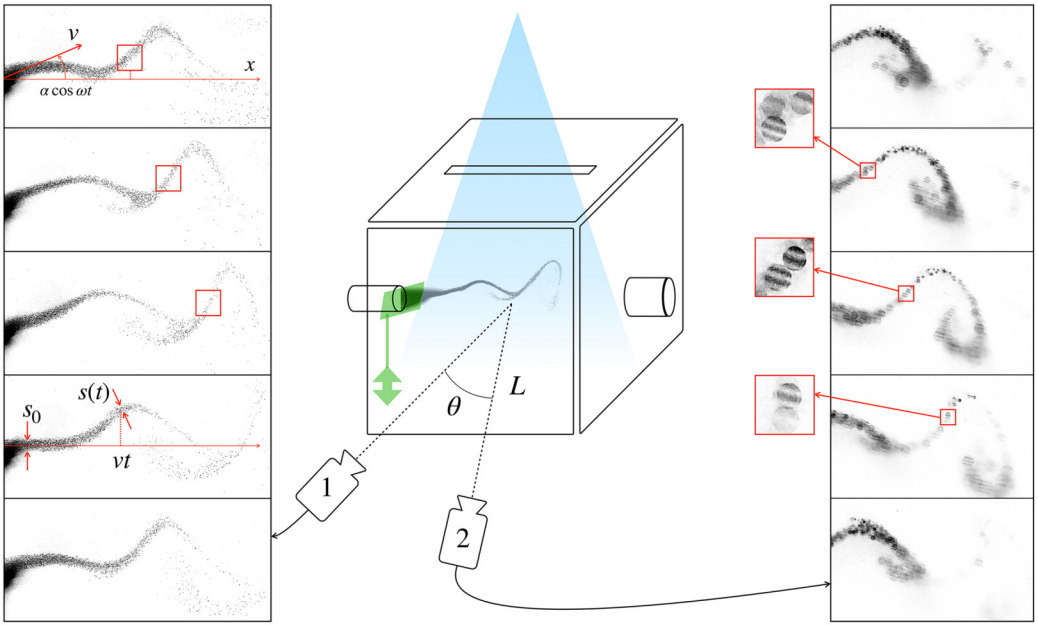

FIG. 1. A large ($35 \times 35 \times 35\,\mathrm{cm}^3$) box safe from droughts is fitted with an inlet for the spray injection, an evacuation outlet on the opposite side, and a slit at the top to let a vertical laser sheet shine through (wavelength $\lambda = 488$ nm). The spray jet (5 mm in diameter) impacts and spreads transversely on a $5 \times 7\,\mathrm{cm}^2$ wide, 0.1-mm-thick glass plate inclined at approximately 10°, thus forming a lamella which then expands inside the box. The plate is connected to a piston oscillating at $\omega/2\pi = 3$ Hz with a 7 mm amplitude, thus conferring to the lamella a weak oscillatory ejection direction of angle $\alpha \cos \omega t$ at a velocity of the order of $v \approx 0.1\,\mathrm{m\,s}^{-1}$. Left: Definition of the residence time of the lamella in the box (featuring a water spray over one oscillation period), and of its thickness $s(t)$ recorded by a camera (1) aiming at right angle with respect to the box transparent wall. Right: The IPI rendering of the same phenomenon recorded by camera (2) aiming at an angle $\theta = 70°$, now visualizing each individual droplet in the spray as a disk featuring a number of stripes proportional to its diameter. Both the kinematics of the lamellae and their drop sizes number and distribution can be documented simultaneously.

a pneumatic atomizer in a nearby separate chamber identical to the one used in [36]: The spray is made of densely packed droplets with sizes of the order of a few to about ten microns which recirculate vigorously into the chamber where they are formed and where they have time to be in equilibrium with their vapor before exiting the chamber. The spray is then conveyed toward the box inlet via a 5-mm-diameter tube. The spray jet impacts and spreads transversely on a $5 \times 7\,\mathrm{cm}^2$ wide, 0.1-mm-thick glass plate inclined at approximately 10°, thus forming a lamella with thickness $s_0 = 3$ mm which then expands inside the box. The plate is connected to a piston oscillating at 3 Hz with a 7 mm amplitude, thus conferring to the lamella a weak oscillatory ejection direction. The spray jet velocity is of the order of $v \approx 0.1\,\mathrm{m\,s}^{-1}$, corresponding to a jet Reynolds number vs_0/ν of about 10 (the viscosity of air is of order $\nu \sim 10^{-5}\,\mathrm{m}^2/\mathrm{s}$), a value too small to sustain the jet Kelvin-Helmoltz instability [41], but large enough to make the lamella sensitive to slight perturbations, explaining the formation of roll-up vortices at the late stage of its development in the box where its expansion is no longer ballistic, but stronger than linear in time. This effect is interesting in itself, and is discussed in Sec. III C. The flow is, however, fairly two-dimensional, the motions being confined to the plane defined by the oscillating piston axis and the jetting direction. We have checked (using Particle Image Velocimetry (PIV) with a mist of nonvolatile oil, see [42]) that the flow velocity field $\mathbf{u}$ in that plane is such that $|\nabla \mathbf{u}| \approx 0$, more precisely that $|\nabla \mathbf{u}/\nabla \times \mathbf{u}| \lesssim 10^{-1}$ in all instances. Overall,

TABLE I. Physical properties of fluids at $T = 293$ K. The density of the liquid is ρ_l, and M is the molecular mass. The saturation density derives from the vapor pressure as $\rho_s = Mp_s/\mathcal{R}T$ with $\mathcal{R} = 8.31\text{J}/(\text{mol K})$. Diffusion coefficients D refer to diffusion in air. Propylene glycol values are from [43].

	ρ_l (kg m^{-3})	p_s (Pa)	M (kg mol^{-1})	ρ_s (kg m^{-3})	D (m^2 s^{-1})	σ (mN m^{-1})
Propylene glycol	1040	10.6	76×10^{-3}	0.00034	8.79×10^{-6}	38.57
Water	1000	2340	18×10^{-3}	0.017	2.8×10^{-5}	72.8
Ethanol	789	7410	46×10^{-3}	0.13	1.3×10^{-5}	22.27
Acetone	791	22800	58×10^{-3}	0.5	1.2×10^{-5}	23.7

the stretching rate $\gamma(t)$ along the sheet, with t a Lagrangian marker related to the downstream position x by $t = x/v$, is given by

$$\gamma(t) = \frac{\dot{\ell}}{\ell} = \frac{\sigma}{1+\sigma t} \sim t^{-1}, \tag{2}$$

and is about $10\,\text{s}^{-1}$ at the oscillating plate lip, to decay down to $5\,\text{s}^{-1}$ a few centimeters downstream. The stirring motion measured by the stretching rate of material lines gradually slows down in time.

B. Liquids and diagnostics

The same experiments have been repeated with four different liquids (all listed in Table I), covering a broad range of volatilities, of which the saturation pressure p_s at 20 °C is a measure: Propylene glycol has a very low saturation pressure, droplets practically do not evaporate in the temporal window of observation, and the corresponding mist is used for PIV measurements. At the other extreme, acetone is strongly volatile, and it takes barely one oscillation period of the sheet for the entire spray to vanish (Fig. 2). The liquids have similar magnitudes of surface tensions (meaning that they are fragmented similarly by the pneumatic atomizer) and their vapor also has a very similar diffusion coefficient in air. When mixtures between two components, say 1 and 2, were used (propylene clycol with water or ethanol with water), the resulting saturation pressure was computed from Raoult's law as $\chi p_{s,1} + (1-\chi)p_{s,2}$ with χ the mole fraction of component 1. Two kinds of diagnostics were simultaneously performed:

(1) A first camera is positioned at a right angle from the box front panel to record the kinematics of the undulating lamella, intercepted by a laser sheet shining through the box, perpendicularly to the ejection direction (Fig. 1). From these observations, the lamella transverse thickness $s(t)$ and length $\ell(t)$ between two consecutive nodes are recorded. The lamellae thickness is tracked automatically in windows like the ones displayed in Fig. 2. The uncertainty on $s(t)$ is of the order of the interdroplets distance, implying a relative error reflected by the dispersion of the data points in Fig. 4(a).

(2) The same laser is used to produce interferences between the light paths from the reflection/refraction of its monochromatic light on/through the (spherical) droplets, now recorded by a second camera at an angle with respect to the laser sheet. The method is called Interferometric Particle Imaging (IPI) (see [44,45]). The observable is a number of fringes n associated with each droplet in the spray (provided it is not too dense), this number being related to the droplet diameter d by

$$d = n\frac{2\lambda L}{d_a}\left(\cos\frac{\theta}{2} + \frac{m\,\sin\frac{\theta}{2}}{\sqrt{m^2+1-2m\,\cos\frac{\theta}{2}}}\right)^{-1}, \tag{3}$$

where $\lambda = 488$ nm is the laser wavelength, L is the distance between the camera lens and the laser sheet, $d_a = 0.09/2.8$ m the ratio of the lens focal length (90 mm) to the lens aperture $f = 2.8$, $\theta = 70^\circ$ is the angle between the laser sheet and the camera pointing direction, and $m = n_{\text{liquid}}/n_{\text{air}}$

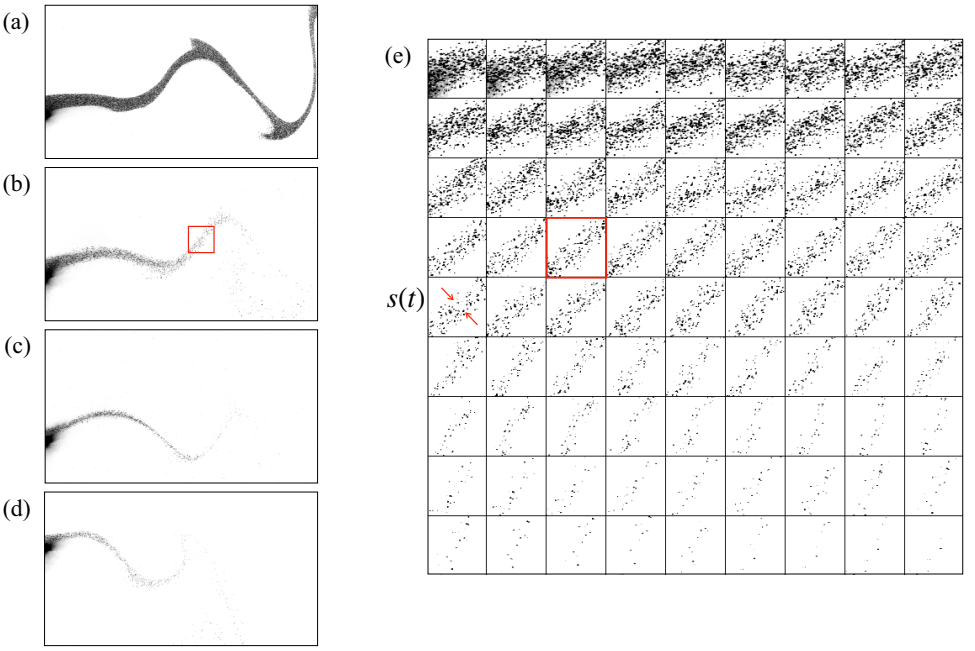

FIG. 2. Snapshots of stirred lamellae about the same oscillation phase, with four different liquids: (a) A solution of propylene glycol mixed with 10% water, (b) water, (c) ethanol, and (d) acetone. The shortening of the lamella persistence length is clearly correlated to the liquid volatility (see Table I). (e) This mosaic shows the Lagrangian evolution of an element of water spray [the abscissa of the red square in (b) is $x = vt$, displaying the shrinking of the lamella, whose topology remains, however, visible down to complete droplets evaporation (from left to right, top to bottom, sampled at every 1/120 second).

is the ratio between the indices of refraction of the liquid to that of air ($m = 1.33/1$ for water/air, there is a different formula when $m < 1$ like for bubbles in water).

With these operating parameters, this concomitant IPI observation allows us to monitor the droplets number of the spray and their size distribution in the range 2-3 μm to 50 μm (the detection limits of the method), as the spray evaporates. A few thousand droplets are typically analyzed individually [see Fig. 7(a)], and an automatic detection procedure allows us to select those diffraction pattern which are not blurred by the superposition with the one of neighboring droplets only [42], and count the fringes.

III. LAMELLA DYNAMICS

A spray lamella is distorted by the stirring motions of the flow at the same time the droplets it carries convert into vapor. The lamella width $s(t)$, notably its decay rate $\dot{s}/s$, is sensitive to the kinematic stretching rate $\gamma(t)$ it experiences in the flow, as well as to the rate at which the vapor is evacuated from its core by molecular diffusion into the diluting environment. We have explained and quantified in [36] that, when the spray is dense and composed of small droplets, the dynamics of the droplets lamella width $s(t)$ is given by

$$\dot{s} = -\gamma(t)s - \frac{\rho_s - \rho_\infty}{\rho}\frac{2D}{\eta(t)}, \tag{4}$$

where ρ_s and ρ_∞ denote the densities of the vapor in the spray lamella core and far outside of it, respectively, and $\rho = \varphi\rho_l + (1-\varphi)\rho_s$ is the total density of the evaporating compound (liquid with volume fraction φ + vapor) in the spray, usually close to the diluting medium density in the absence

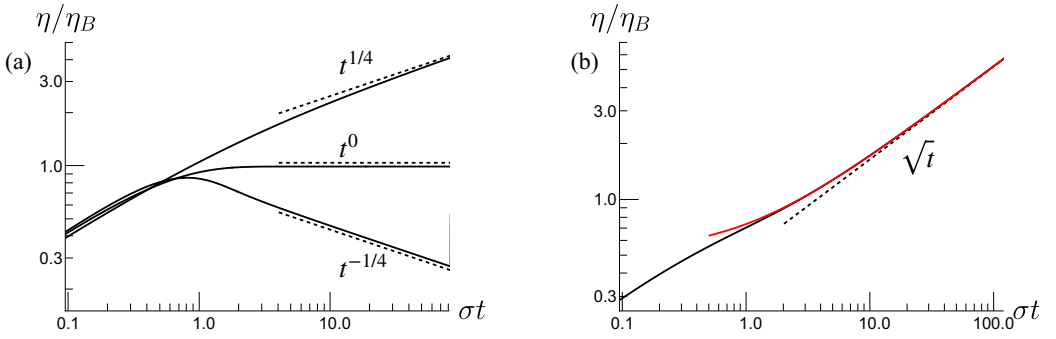

FIG. 3. Generalized Batchelor scales: (a) The length scale $\eta(t)$ computed from Eq. (5) using the generic stretching law in Eq. (6) and scaled by η_B in Eq. (7) for $\beta = 1/2,\ 1,$ and $3/2$. The dashed lines indicate the corresponding power-law dependencies $\eta(t) \sim \eta_B(\sigma t)^{(1-\beta)/2}$ in Eq. (8). (b) The power law stretching studied here in Eq. (2) gives a generalized Batchelor scale tangent to $\eta(t) \sim \sqrt{D(t+\sigma^{-1})}$ in Eq. (9) after the mixing time (red line), growing asymptotically like $\sqrt{Dt}$ (dashed line).

of buoyancy effects. The relative humidity ρ_∞/ρ_s is zero for organic substances, and of the order of 30% with water. Compared to the pure kinematics $\dot{s} = -\gamma(t)s$ reflecting substrate deformation, the additional ablation term in Eq. (4) stands for the droplets close to the lamella edge which, when exposed to the fresh diluting environment, evaporate on a timescale given by the d-squared law, short in front of $\gamma(t)^{-1}$. The length scale $\eta(t)$, a generalized Batchelor scale, is the thickness of the vapor concentration gradient on each side of the lamella (hence the factor 2).

A. The generalized Batchelor scale

The vapor diffuses with diffusion coefficient D across a concentration gradient of thickness $\eta(t)$, itself a function of the stretching intensity $\gamma(t)$. This ablation term has a structure similar to the one of the d-squared law, where $\eta(t) \sim d$ for a droplet of size d evaporating in a quiescent environment [2], or $\eta(t) \sim \mathrm{Re}^{1/2}\mathrm{Sc}^{1/3}$ when the droplet has a relative velocity u at Reynolds number $\mathrm{Re} = ud/\nu$ and $\mathrm{Sc} = \nu/D$ is the vapor Schmidt number [10]. For a given stirring protocol setting $\gamma(t)$, Eq. (4) is solved in a closed form since we have (see Eqs. (7) and (8) in [36], an application to sprays in [37] and also [46] for a general discussion)

$$\eta(t) = \exp\left(-\int_0^t \gamma(t')\mathrm{d}t'\right)\sqrt{D\int_0^t \mathrm{d}t' \exp\left(2\int_0^{t'} \mathrm{d}t''\gamma(t'')\right)}. \tag{5}$$

The length scale $\eta(t)$ is a generalized Batchelor scale [47] resulting from the—possibly unbalanced—equilibrium between substrate compression and diffusive broadening. For the sake of illustration, let us consider as in [36] a family of generic stretching rates parametrized by an exponent β:

$$\frac{\gamma(t)}{\sigma} = \beta(\sigma t)^{\beta-1}. \tag{6}$$

Stretching weakens in time when $\beta < 1$, and reinforces for $\beta > 1$. The original Batchelor scale

$$\eta(t) \equiv \eta_B \sim \sqrt{\frac{D}{\sigma}} \tag{7}$$

corresponds to $\beta = 1$ when the stretching rate is constant in time, leading to an exponential increase of material line lengths ℓ. From Eq. (5) using (6), one finds that

$$\eta(t) \xrightarrow[\sigma t \gg 1]{} \sqrt{\frac{D}{2\beta\sigma}} (\sigma t)^{\frac{1-\beta}{2}}, \tag{8}$$

and Fig. 3(a) shows how compression is too slow to overcome diffusion when $\beta < 1$ leading to a broadening of $\eta(t)$, and vice versa when $\beta > 1$. Strict equilibrium is only reached for $\beta = 1$.

When the stretching rate $\gamma(t)$ decays algebraically in time as in Eq. (2) which suits the present study, one finds that $\eta(t)$ coincides, after a mixing time of the order of σ^{-1} [46], with [Fig. 3(b)]

$$\eta(t) = \sqrt{\frac{D(t+\sigma^{-1})}{1+2\beta}}, \tag{9}$$

increasing proportionally to the standard diffusion length $\sqrt{Dt}$.

B. Predictions for a linear elongation

Using $\eta(t) \sim \sqrt{D(t+\sigma^{-1})}$ and further counting time t from $t = \sigma^{-1}$ in units of σ^{-1} to form $\mathcal{T} = 1 + \sigma t$, we have from Eq. (4) for $\mathcal{S} = s/s_0$,

$$\dot{\mathcal{S}} = -\frac{\mathcal{S}}{\mathcal{T}} - \frac{\phi}{\sqrt{\mathcal{T}}}$$

$$\text{where} \quad \phi = \frac{\rho_s - \rho_\infty}{\rho} \frac{2}{\sqrt{\text{Pe}}} \quad \text{and} \quad \text{Pe} = \frac{\sigma s_0^2}{D}, \tag{10}$$

whose solution with $\mathcal{S}(1) = 1$, a boundary condition expressing that $s = s_0$ at $t = 0$, is

$$\mathcal{S} = \frac{3 + 2\phi - 2\phi\,\mathcal{T}^{3/2}}{3\mathcal{T}}. \tag{11}$$

The lifetime $t_\star$ of the spray lamella, defined when all the liquid it carries has been transferred into vapor, itself evacuated from its core by stretching enhanced diffusion, namely, when $\mathcal{S}(t_\star) = 0$, is given by

$$\sigma t_\star = \left(1 + \frac{3}{2\phi}\right)^{2/3} - 1 \xrightarrow[\phi \ll 1]{} \left(\frac{3}{2\phi}\right)^{2/3}. \tag{12}$$

The trajectories of $\mathcal{S}$ as a function of time are displayed in Fig. 4(a) for sprays with liquids spanning a broad range of volatilities (see Table I). All sprays were prepared identically with $s_0 = 3\,\text{mm}$, lamella elongation rates in the range $\sigma \sim 2 - 5\,\text{s}^{-1}$, and with Péclet numbers slightly above unity (Pe ≈ 5 for a 10% polyethylene-Gglycol/water mixture and pure water and Pe ≈ 10 for pure acetone and ethanol), corresponding to values of ϕ barely smaller than unity, suggesting that the validity domain of the above theory for the present experiments is only marginal. Nevertheless, the scaling in Eq. (12) first collapses all the lifetimes for the different liquids on a master curve [Fig. 4(b)], and, second, fits the data well, in scaling law and absolute value on the whole range of ϕ, even, surprisingly, when it is larger than unity.

A dense spray lamella evaporation time, or lifetime is of order of the substrate elongation rate ($t_\star \sim \sigma^{-1}$), is relative to the d-squared law weakly dependent on the volatility of the liquid droplets it carries ($t_\star \sim \rho_s^{-2/3}$), is independent of the size d of the droplets, and is very weakly dependent of its vapor diffusivity ($t_\star \sim D^{-1/3}$). By contrast, the d-squared droplet lifetime $t_1 = d^2/(8D) \times \rho_l/(\rho_s - \rho_\infty)$ depends strongly on the droplets size, is independent of σ, and presents much stronger dependencies on the thermodynamic/diffusive characteristics of the liquid/vapor at play than $t_\star$ does. The present lamella have lifetimes $t_\star$ of the order of 0.3−3 s while the d-squared t_1 calculated as in

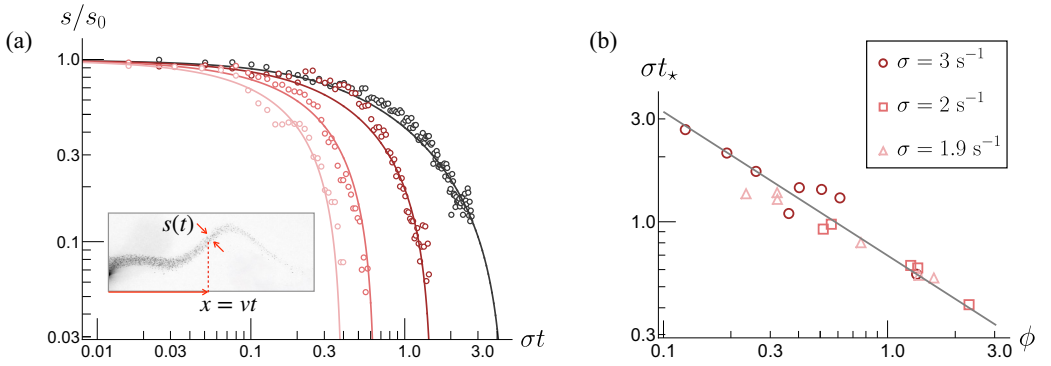

FIG. 4. Kinematics and lifetimes: (a) Lamellae thickness $\mathcal{S} = s(t)/s_0$ recorded as a function of σt for $\sigma = 2\,\mathrm{s}^{-1}$ with different liquids. From dark to light tones in decreasing order of lamellae persistence: A mixture of propylene glycol with 10% water ($\phi = 0.12$), water ($\phi = 0.25$), ethanol ($\phi = 0.75$), and acetone ($\phi = 1.2$). The continuous lines are the parameter-free fits given by Eq. (11). (b) The corresponding lamellae lifetimes obtained for different values of σ and liquids, as a function of ϕ and fit by Eq. (12).

[36] would be in the range $10^{-2}-10^{-1}$ s for droplets with size of the order of 5 μm (see Fig. 4 and Sec. IV).

C. Superlinear elongations

The lamella is a plane, two-dimensional jet moving in a quiescent environment, and as such is liable to sustain a sinusoidal mode of instability which is damped but not canceled by viscosity [48,49]. Although the lamellae Reynolds number, of the order 10, is weak, that instability, hastened by the oscillating injection conditions at the plate lip, is clearly visible, forming roll-up vortices inducing a faster than linear increase of material lines along the lamella. A qualitatively similar phenomenon was noticed in [36]. The consequence of this superlinear elongation is obviously to accelerate the evaporation of the spray.

Writing that the effective stretching rate is, for instance, $\gamma(t) = \beta\sigma/(1+\sigma t)$, or $\gamma/\sigma = \beta/\mathcal{T}$ with $\beta > 1$ for a superlinear elongation (corresponding to an elongation $\ell/\ell_0 = (1+\sigma t)^\beta$), the lamella width dynamics in Eq. (10) becomes

$$\dot{\mathcal{S}} = -\beta\frac{\mathcal{S}}{\mathcal{T}} - \frac{\phi}{\sqrt{\mathcal{T}}} \tag{13}$$

since the vapor concentration gradient at the edge of a lamella $\eta(t) \sim \sqrt{D(t+\sigma^{-1})}$ remains unchanged compared to the case of a linear elongation as seen from Eq. (9). The solution to Eq. (13) is now $\mathcal{S} = (1 + 2\beta + 2\phi - 2\phi\mathcal{T}^{\frac{1}{2}+\beta})/([1+2\beta]\mathcal{T}^\beta)$, corresponding to a lamella lifetime

$$\sigma t_\star \underset{\phi\ll 1}{\longrightarrow} \phi^{-\frac{2}{2\beta+1}}, \tag{14}$$

even lesser dependent on the thermodynamic/diffusive properties of the mixtures when $\beta > 1$. Such occurrences are encountered in the final roll-up phase of the vortex formed at large time after the lamellae linear elongation phase, with typically $\beta = 1.3$, as seen in Fig. 5(a). In fact, in the same way that there is a distribution of Lyapunov exponents, or effective stretching rates, in turbulent flows (see, e.g., [50] and references thererin), there is a distribution of β in the roll-up phase at late times. Even exponential stretchings, as those typical of larger Reynolds number shear flows, considered in [36], do occur here in the late lamellae folding phase, as seen in Fig. 5(b). These events, described by $\dot{\mathcal{S}} = -\mathcal{S} - \phi$ leading to $\mathcal{S} = (1+\phi)e^{-\mathcal{T}} - \phi$, are characterized by an even weaker dependence

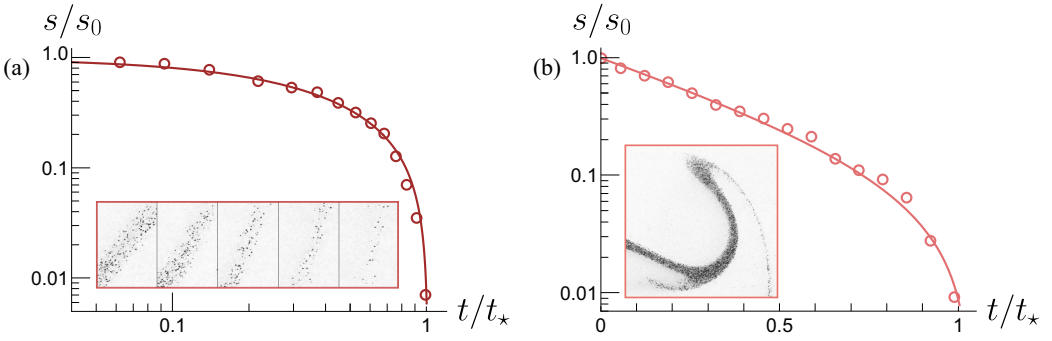

FIG. 5. Superlinear elongations. (a) A water lamella ruled by Eq. (13) with $\beta = 1.3$. (b) An ethanol lamella with $\phi = 0.09$ in the late folding phase experiencing an exponential-like stretching $\mathcal{S} = (1+\phi)e^{-\mathcal{T}} - \phi$.

of the evaporation time on the thermodynamic/diffusive properties of the liquid/vapor, that is, on ϕ in Eq. (10), since in that case $\sigma t_\star \sim -\ln\phi$.

IV. DROPLETS NUMBER AND SIZE DISTRIBUTION

The evaporation of dense sprays is a mixing process, not reducible to the dynamics of its elementary constituents—the droplets—taken in isolation. By dense, we mean sprays where the typical interdroplets separation distance is smaller than the enrichment length ℓ_e defined as the diameter of the sphere containing at concentration ρ_s all the vapor of an evaporated droplet, such that $\rho_\infty \ell_e^3 + \rho_l d^3 = \rho_s \ell_e^3$, that is [36],

$$\ell_e \sim d\left(\frac{\rho_l}{\rho_s - \rho_\infty}\right)^{1/3}, \tag{15}$$

which, for water in usual ambient conditions, is about 40 times the initial droplet diameter d. There is initially about $N = \int n(d,0)\mathrm{d}d \approx 10^3$ [see Fig. 7(a)] microns in size droplets stacked across a lamella width whose transverse size s_0 is a few millimeters, so the criterion for dense is largely met. The group evaporation number Nd/s_0 introduced by [18] is, accordingly, larger than unity indicating that droplets at the core of the lamella are surrounded by their saturation vapor, preventing them from evaporation. Only those droplets which are close to the lamella border are exposed to a dryer environment, and when it happens that a droplet escapes from the lamella, it evaporates on a timescale given by the d-squared law based on its exit diameter, as seen in Fig. 6.

Droplets sizes are distributed in sprays. The question we want to examine now concerns the evolution the Probability Density Function (PDF) of the droplets sizes $p(d,t)$ during the lamella evaporation, that is, for t running from 0 to $t_\star$. Let us envisage two extreme scenarii, one—alas still popular—reflecting the isolated droplet limit, the other being inspired by the present observations:

(1) Consider the dilute limit (irrelevant to most natural sprays, as recalled in Sec. I) where droplets are separated by a distance much larger than ℓ_e, and evaporate independently according to the d-squared dynamics [2,5]

$$d = \sqrt{d_0^2 - \kappa t}, \tag{16}$$

with $\kappa \sim D\rho_s/\rho_l$ and d_0 an initial size. Let $p(d_0,0)$ be the initial distribution of droplets sizes d_0 in this assembly. Obviously, small droplets will disappear sooner than larger ones. Consider a range of droplets sizes around d, still alive at time t. Since the sizes d have been simply transported from their initial value d_0 by the d-squared transformation in Eq. (16), we have, by probability conservation,

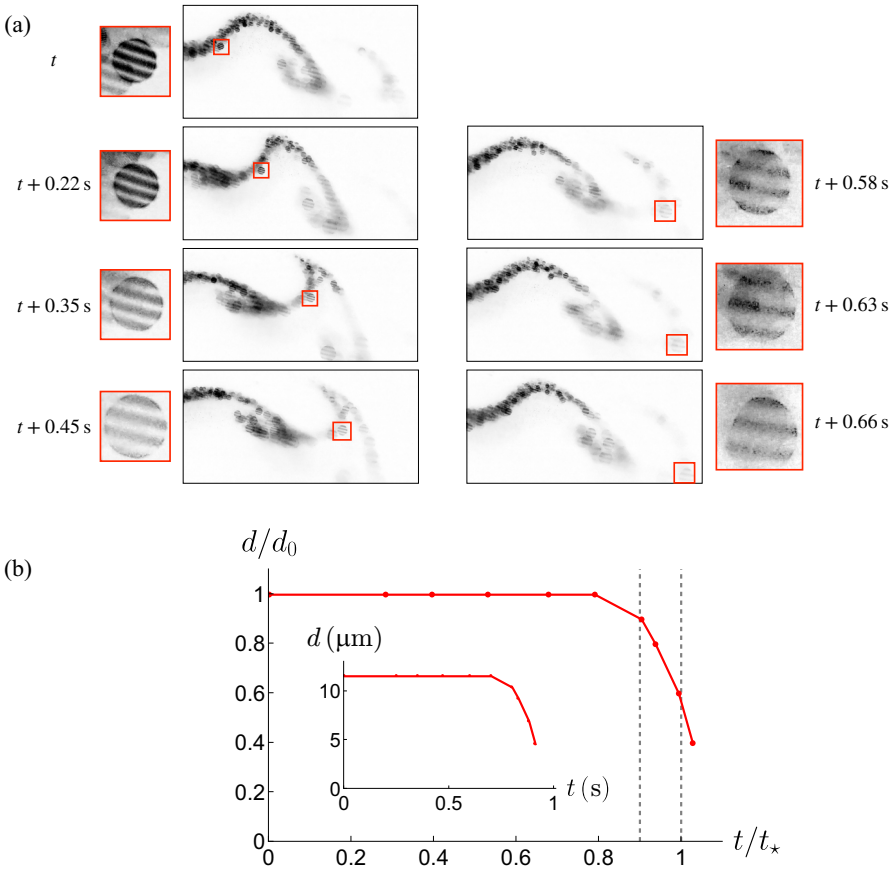

FIG. 6. The Lagrangian history of a droplet in a dense water spray, from its injection close to the lamella border up to near its disappearance ($t_\star \approx 0.9$ s), along with the evolution of its size, showing the acceleration of the droplet diameter decay as a function of time. (a) IPI snapshots of the droplet at increasingly shorter time intervals. (b) Temporal evolution the droplet diameter measured by IPI illustrating how, as soon as it has left the spray core, it evaporates on a timescale of the order of 0.08 s as expected from the d-squared law (the interval between the dashed vertical lines).

stating that $p(d,t)\mathrm{d}d = p(d_0,0)\mathrm{d}d_0$:

$$p(d,t) = \frac{d}{\sqrt{d^2+\kappa t}}\, p(\sqrt{d^2+\kappa t},0)$$

$$\text{or} \quad p(d \ll \sqrt{\kappa t},t) \sim \frac{d}{\sqrt{\kappa t}}\, p(\sqrt{\kappa t},0)$$

$$\text{and} \quad p(d > \sqrt{\kappa t},t) \sim p(d,0). \tag{17}$$

The large excursion wing of the PDF (where sizes are greater than $\sqrt{\kappa t}$) is left practically unchanged at time t, while its low sizes inner tail is such that $p(d,t) \sim d$. The isolated droplets scenario thus predicts that the PDF will deform as evaporation proceeds toward a universal shape tangent to d for $d < \sqrt{\kappa t}$, reflecting the acceleration of the droplets decay as they gets smaller.

This negatively skewed (i.e., with a fat tail on the small sizes side) distribution shape is reminiscent of the distribution obtained through Ostwald ripening, a phenomenon explained by the

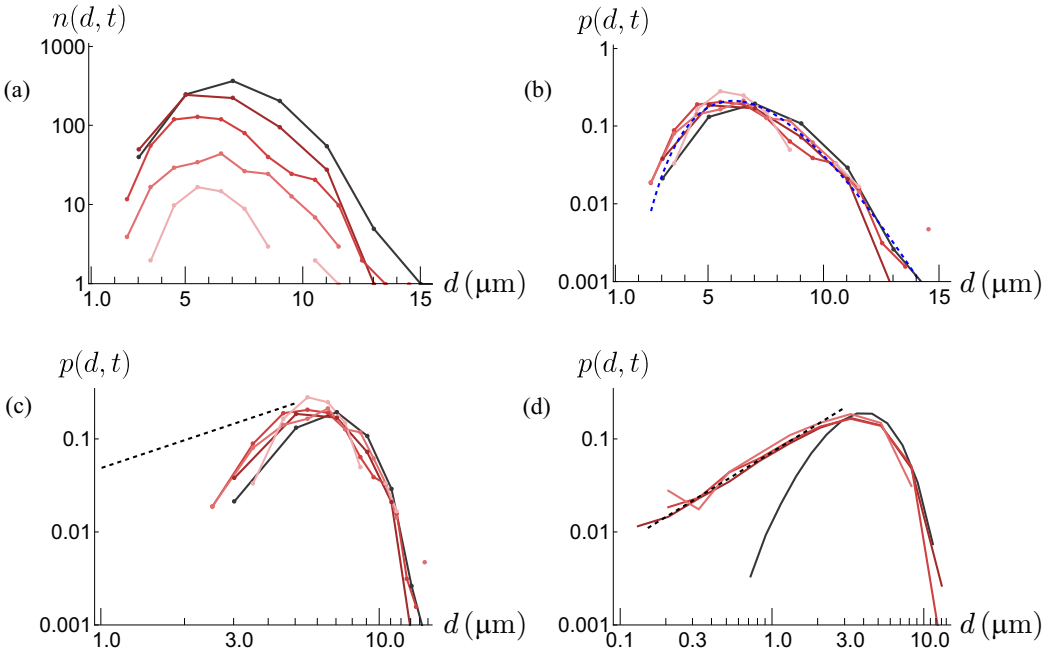

FIG. 7. Evolution of the drop number and size distribution in a water spray ($\sigma t_\star \approx 1.38$). (a) Number of droplets per diameter class $n(d,t)$ at successive instants of time $t = 0.04, 0.1, 0.2, 0.28, 0.36$ s (from dark to light tones) for $\sigma = 3\,\mathrm{s}^{-1}$. (b) The corresponding size distribution $p(d,t)$. (c) Same as in (b) in log-log units, emphasizing the small sizes shape of $p(d,t)$, and the invariance of the distribution in time [Eq. (18)]. (d) Evolution of $p(d,t)$ with the same initial condition $p(d,0)$ as in (c) drawn by the black line, under the isolated droplets scenario, showing the emergence of the $p(d,t) \sim d$ [Eq. (17)] small sizes tail of the distribution, clearly absent in (c).

Lifshitz-Slyozov mechanism [51]. In that mechanism, the saturation pressure $p_s(d)$ at the surface of small droplets being larger than at the surface of larger ones (Kelvin's correction), a flux where big drops grow at the expense of smaller ones by vapor diffusion in the substrate, is sustained; droplets interact via the vapor phase. Kelvin's correction is, however, only sensible for very small droplets: If p_s is the vapor pressure for a flat interface (Table I), then $p_s(d) = p_s e^{-d_\star/d}$ with $d_\star \sim M\sigma/\rho_l RT \approx 10^{-8}$ m (for water). This mechanism is nevertheless claimed to be relevant in various instances involving much larger droplets [52,53]. The mechanism described here, although giving rise to a qualitatively similar phenomenology (the negative skewness), is fundamentally different since it only relies on the acceleration of a droplet diameter cancellation as it approaches zero, the droplets being otherwise independent in the spray.

(2) In the dense spray limit, the distribution $p(d_0, 0)$ is uniformly sampled within the spray. To a first approximation, there is no segregation of sizes across the lamella and there is no reason to find bigger or smaller droplets anywhere in it. It is only when a drop is hit by the receding boundary of the lamella that it evaporates, and this event is independent of its size. Therefore, the vapor mixing scenario we have described so far predicts, by contrast with the isolated droplets scenario, that the PDF will remain unchanged during the evaporation of the lamella

$$p(d,t) = p(d,0), \tag{18}$$

although the number of droplets per diameter class $n(d,t)$ and consequently the net droplets number still alive $\int n(d,t)\mathrm{d}d$ decreases in time, with an evolution parallel to the one of $s(t)$.

The PDF $p(d, t = x/v)$ were measured by the IPI technique explained in Sec. II B and averaged over a large number of water droplets passing through a fixed window at successive downstream locations $x = vt$. As expected, the number $n(d, t)$ of still alive droplets is a decreasing function of x (i.e., of t), but their size distribution $p(d, t) = n(d, t)/\int n(d, t)\mathrm{d}d$ is closer to invariant than tending toward the shape $p(d) \sim d$ predicted by the d-squared law. Also, the mean droplets diameter $\langle d\rangle = \int d\, p(d, t)\mathrm{d}d \approx 5\,\mu\mathrm{m}$ remains approximately constant as the droplets number decays, down to complete evaporation (Fig. 7) suggesting that the mixing scenario, as opposed to the d-squared law, is indeed appropriate to describe the droplets population of the present dense sprays. Even more convincingly, if the diameter of each droplet in the initial number density distribution $n(d, 0)$ is forced to evolve according to Eq. (16) and the current distribution $p(d, t)$ is calculated for subsequent times, one sees that the PDF trajectory, notably the emergence of its negatively skewed shape, is markedly different from the one actually observed (which is invariant).

The fates of droplets embedded in a spray evolving in the dilute, and dense limits are clearly distinguishable. For instance, *in situ* measurements at the border of clouds exhibit the coexistence of dense, water vapor rich regions carrying a large amount of droplets and dilute, droplet-free regions, separated by sharp boundaries [54]. Numerical simulations also show that a population of sparse droplets evaporates according to a scenario closer from Eq. (17) with the progressive emergence of a clear negative skewness tail [55].

V. CONCLUSION

Small droplets do not evaporate faster than bigger ones in a dense spray, which itself lives much longer than if its constituents were isolated.

This paradigm, formalized in Eqs. (4), (5), and (18), should certainly be considered seriously in a number of applications, including those evoked in Sec. I. Its implementation requires knowledge of the stirring protocol involved in the vapor field mixing, namely, the value of $\gamma(t)$ at every point in the medium, a quantity which is computed from the deformation tensor of the underlying stirring field [56]. Mild stirring, as in the present experiments, often involves temporal power law stretchings of material lines, and in that case the persistence time $t_\star$ of the spray is given by Eq. (14). Strong stirring like in turbulent flows with exponential stretching at constant rate γ implies that $\gamma t_\star \sim -\ln\phi$. In all cases, the volatility of the liquid, its volume fraction in the spray, the relative humidity in the diluting medium and the diffusion coefficient of the vapor are embedded in a the single number ϕ defined in Eq. (10). This number is smaller than unity when the Péclet number of the flow is large, the condition of applicability of the mixing scenario depicted here and in our previous contributions on the subject [36,37].

Like stretched scalar lamellae are the quanta of complex mixtures, the spray lamella is the elementary brick of any dense spray. However, two supplementary ingredients need to be considered when exporting these idea to the real world:

First, flows present a typically broad distribution of stretching rates γ (or Lyapunov exponents in the language of turbulence) and hence a distribution of lifetimes $t_\star$ like there is a distribution of mixing times in random flows [46]. For instance, Fig. 8 shows an instantaneous planar laser cut through an impulsive water spray (a puff), revealing its internal organization as a set of unevenly stretched (reflecting the distribution of γ), sparse lamellae, surrounded by fresh dry regions from the outside dry medium. This ingredient, notably the existence of low stretching rates, obviously conditions the overall lifetime of the puff.

Second, close-by spray lamellae which may possibly be brought in the proximity of each other in convergent regions of the flow where their diffusive boundaries may overlap and thus hinder their respective evaporation, as droplets in the spray do among themselves, will result in a further delay for evaporation. The relative importance of this effect needs to be determined on a case by case basis.

While it succeeds at solving an evaporation problem in a simple configuration, it remains to be seen how this lamellar concept can solve nontrivial problems in complex sprays. There are already

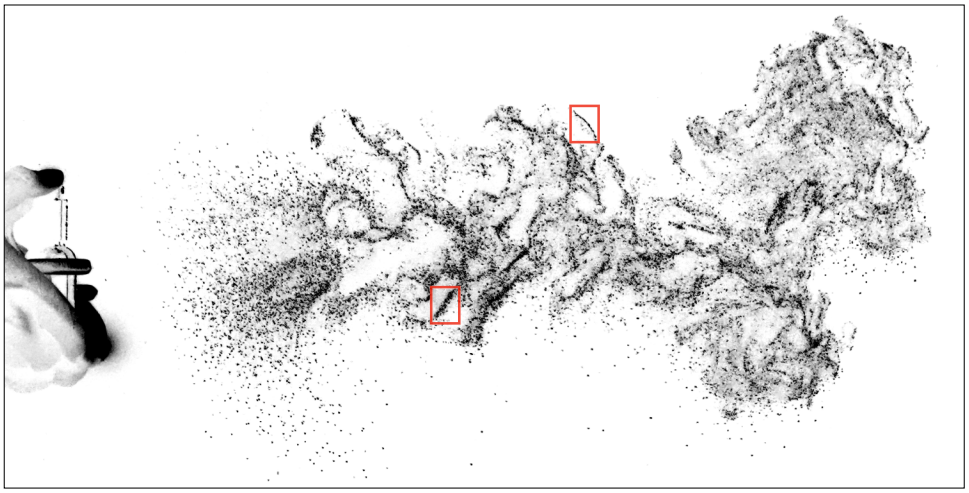

FIG. 8. An instantaneous planar laser cut through an impulsive water spray produced by a hand held atomizer, revealing its architecture: Unevenly stretched sparse lamellae are surrounded by droplet free regions incorporated from the outside dry medium. The two lamellae highlighted in the spray, one thicker than the other, have different elongations histories.

encouraging signs [57] that this method is an efficient alternative to direct numerical simulations in the large Péclet number limit, like in turbulent flows carrying a vapor field in interaction with evaporating droplets.

DATA AVAILABILITY

The data that support the findings of this article are not publicly available. The data are available from the authors upon reasonable request.

[1] L. D. Landau and E. M. Lifschitz, *Statistical Physics, Part 1* (Pergamon Press, Oxford, 1980), Vol. 5.
[2] I. Langmuir, The evaporation of small spheres, Phys. Rev. **12**, 368 (1918).
[3] H. W. Morse, On evaporation from the surface of a solid sphere, Proc. Am. Acad. Arts Sci. **45**, 363 (1910).
[4] H. G. Houghton, A study of the evaporation of small water drops, J. Appl. Phys. **4**, 419 (1933).
[5] W. E. Ranz and W. R. Marshall, Evaporation from drops, Part I, Chem. Eng. Progr. **48**, 141 (1952).
[6] A. L. Sanchez, J. Urzay, and A. Linan, The role of separation of scales in the description of spray combustion, Proc. Combust. Inst. **35**, 1549 (2015).
[7] A. S. Rana, D. A. Lockerby, and J. E. Sprittles, Lifetime of a nanodroplet: Kinetic effects and regime transitions, Phys. Rev. Lett. **123**, 154501 (2019).
[8] J. Finneran, C. P. Graner, and F. Nadal, Deviations from classical droplet evaporation theory, Proc. R. Soc. A **477**, 20210078 (2021).
[9] P. S. Epstein and M. S. Plesset, On the stability of gas bubbles in liquid-gas solutions, J. Chem. Phys. **18**, 1505 (1950).
[10] W. E. Ranz and W. R. Marshall, Evaporation from drops, Part II, Chem. Eng. Progr. **48**, 173 (1952).
[11] K. V. Beard and H. R. Pruppacher, A wind tunnel inverstigation of the rate of evaporation of small water drops falling at terminal velocity in air, J. Atmos. Sci. **28**, 1455 (1971).
[12] E. Ghabache, G. Liger-Belair, A. Antkowiak, and T. Séon, Evaporation of droplets in a champagne wine aerosol, Sci. Rep. **6**, 25148 (2016).

[13] F. Veron, C. Hopkins, E. L. Harrison, and J. A. Mueller, Sea spray spume droplet production in high wind speeds, Geophys. Res. Lett. **39**, 2012GL052603 (2012).
[14] E. R. Baylor, M. B. Baylor, D. C. Blanchard, L. D. Syzdek, and C. Appel, Virus transfer from surf to wind, Science **198**, 575 (1977).
[15] G. J. Dorr, A. J. Hewitt, S. W. Adkins, J. Hanan, H. Zhang, and B. Noller, A comparison of initial spray characteristics produced by agricultural nozzles, Crop Prot. **53**, 109 (2013).
[16] E. Villermaux, Fragmentation versus cohesion, J. Fluid Mech. **898**, P1 (2020).
[17] T. Varkenvisser, S. Kooij, E. Villermaux, and D. Bonn, Effect of high wind speeds on droplet formation in sprays, J. Fluid Mech. **1000**, A86 (2024).
[18] H. H. Chiu and T. M. Liu, Group combustion of liquid droplets, Combust. Sci. Technol. **17**, 127 (1977).
[19] N. Chigier, Group combustion models and laser diagnostic methods in sprays: A review, Combust. Flame **51**, 127 (1983).
[20] R. C. Srivastava, Growth of cloud drops by condensation: A criticism of currently accepted theory and a new approach, J. Atmos. Sci. **46**, 869 (1989).
[21] H. R. Pruppacher and J. D. Klett, *Microphysics of Clouds and Precipitation* (Kluwer Academic Publishers, Amsterdam, 1997).
[22] A. B. Kostinski, Simple approximations for condensational growth, Environ. Res. Lett. **4**, 015005 (2009).
[23] J. Fries, G. Sardina, G. Svensson, A. Pumir, and B. Mehlig, Lagrangian supersaturation fluctuations at the cloud edge, Phys. Rev. Lett. **131**, 254201 (2023).
[24] X. Lefebre, M. Chartray-Pronovost, C. Duchaine, E. Bédard, M. Prévost, and E. Robert, Evaporation of aerosol droplets from contaminated cooling tower water, Phys. Fluids **37**, 023365 (2025).
[25] E. J. Lowbury, The persistence of dust in occupied rooms, Epidemiol. Infect. **48**, 1 (1950).
[26] J. P. Duguid, The size and the duration of air-carriage of respiratory droplets and droplet-nuclei, Epidemiol. Infect. **44**, 471 (1946).
[27] C. E. Turner, M. W. Jennison, and H. E. Edgerton, Public health applications of high-speed photography, American Journal of Public Health **31**, 319 (1941).
[28] L. Bourouiba, E. Dehandschoewercker, and J. W. M. Bush, Violent expiratory events: On coughing and sneezing, J. Fluid Mech. **745**, 537 (2014).
[29] K. L. Chong, C. S. Ng, N. Hori, R. Yang, R. Verzicco, and D. Lohse, Extended lifetime of respiratory droplets in a turbulent vapor puff and its implications on airborne disease transmission, Phys. Rev. Lett. **126**, 034502 (2021).
[30] F. W. Wells, *Airborne Contagion and Air Hygiene* (Harvard University Press, Cambridge, MA, 1955).
[31] R. L. Riley and F. O'Grady, *Airborne Infection, Transmission and Control* (The MacMillan Company, New York, 1961).
[32] T. Umeki, M. Ohata, H. Nakanishi, and M. Ichikawa, Dynamics of microdroplets over the surface of hot water, Sci. Rep. **5**, 8046 (2015).
[33] G. Castanet, L. Perrin, O. Caballina, and F. Lemoine, Evaporation of closely-spaced interacting droplets arranged in a single row, Int. J. Heat Mass Transfer **93**, 788 (2016).
[34] O. Carrier, N. Shahidzadeh, R. Zargar, M. Aytouna, M. Habibi, J. Eggers, and D. Bonn, Evaporation of water: Evaporation rate and collective effects, J. Fluid Mech. **798**, 774 (2016).
[35] A. Bouillant, J. H. Snoeijer, and B. Andreotti, Collective effects in breath figures, Phys. Rev. Fluids **10**, 053605 (2025).
[36] A. de Rivas and E. Villermaux, Dense spray evaporation as a mixing process, Phys. Rev. Fluids **1**, 014201 (2016).
[37] E. Villermaux, A. Moutte, M. Amielh, and P. Meunier, Fine structure of the vapor field in evaporating dense sprays, Phys. Rev. Fluids **2**, 074501 (2017).
[38] W. E. Ranz, Application of a stretch model to mixing, diffusion and reaction in laminar and turbulent flows, AIChE J. **25**, 41 (1979).
[39] P. Meunier and E. Villermaux, How vortices mix, J. Fluid Mech. **476**, 213 (2003).
[40] M. Souzy, I. Zaier, H. Lhuissier, T. Le Borgne, and B. Metzger, Mixing lamellae in a shear flow, J. Fluid Mech. **838**, R3 (2018).
[41] H. A. Becker and T. A. Massaro, Vortex evolution in a round jet, J. Fluid Mech. **31**, 435 (1968).

[42] L. Rotily, The persistance of evaporating dense sprays, Ph.D. thesis, Aix-Marseille University, 2024.
[43] G. A. Lugg, Diffusion coefficients of some organic and other vapors in air, Anal. Chem. **40**, 1072 (1968).
[44] C. Tropea, Optical particle characterization in flows, Annu. Rev. Fluid Mech. **43**, 399 (2011).
[45] N. Semidetnov and C. Tropea, Conversion relationships for multidimensional particle sizing techniques, Meas. Sci. Technol. **15**, 112 (2004).
[46] E. Villermaux, Mixing versus stirring, Annu. Rev. Fluid Mech. **51**, 245 (2019).
[47] G. K. Batchelor, Small-scale variation of convected quantities like temperature in turbulent fluid, Part 1. General discussion and the case of small conductivity, J. Fluid Mech. **5**, 113 (1959).
[48] J. W. Lord Rayleigh, On the stability, or instability of certain fluid motion, Proc. Lond. Math. Soc. **s11-11**, 57 (1880).
[49] H. B. Squire, Investigation of the stability of a moving liquid film, Br. J. Appl. Phys. **4**, 167 (1953).
[50] N. Petropoulos, S. M. de Bruyn Kops, P. Meunier, and E. Villermaux, Lyapunov exponents in conservative systems: The importance of rare compression events (unpublished).
[51] I. M. Lifshitz and V. V. Slyozov, The kinetics of precipitation from supersaturated solid solutions, J. Phys. Chem. Solids **19**, 35 (1961).
[52] J. J. Kilbride, F. F. Ouali, and D. J. Fairhurst, Ostwald ripening in evaporating respiratory breath figures, Phys. Rev. Fluids **10**, L101601 (2025).
[53] M. Tateno and O. A. Saleh, Diffusive and enzymatic modulation of the dynamic size distribution of DNA droplets, Phys. Rev. Lett. **136**, 068403 (2026).
[54] M. J. Beals, J. P. Fugal, R. A. Shaw, J. Lu, S. M. Spuler, and J. L. Stith, Holographic measurements of inhomogeneous cloud mixing at the centimeter scale, Science **350**, 87 (2015).
[55] B. Kumar, J. Schumacher, and R. A. Shaw, Lagrangian mixing dynamics at the cloudy–clear air interface, J. Atmos. Sci. **71**, 2564 (2014).
[56] P. Meunier and E. Villermaux, The diffuselet concept for scalar mixing, J. Fluid Mech. **951**, A33 (2022).
[57] V. Pushenko, S. Scollo, P. Meunier, E. Villermaux, and J. Schumacher, Diffuselet method for three-dimensional turbulent mixing of a cloudy air filament, Phys. Rev. Fluids **10**, 074503 (2025).